

Semiconductor grain-boundary admittance: Theory

G. E. Pike

Sandia National Laboratories, Albuquerque, New Mexico 87185

(Received 7 September 1983)

The electrical admittance due to majority carriers in semiconductor bicrystals is calculated as a function of frequency and applied dc voltage. At low frequencies the admittance is controlled by charge trapping at the grain boundary which modulates the thermionic emission current across the boundary. The admittance does not generally obey a simple Debye-type form, although in most cases it is similar. Examples for the frequency and voltage dependence of the admittance are given for two energy distributions of the grain-boundary trap states.

INTRODUCTION

In polycrystalline semiconductors the electrical transport properties are often dominated by the double depletion-layer structures which form around the grain boundaries.¹⁻¹⁰ Most of the research has concentrated on the dc conductivity due to grain-boundary potential barriers, but some measurements of the frequency-dependent conductance and capacitance have been reported.^{4,9,11-14} As a function of frequency and applied voltage the admittance can be very different from that measured in ordinary dielectric materials.^{4,9,13,14} For example, the low-frequency capacitance of a silicon bicrystal is observed to change by a factor of 25 when a dc voltage of only 0.2 V is applied across the grain boundary.⁴ Only one detailed theoretical treatment of this grain-boundary admittance has been published, and it is limited by the assumptions of a constant density of grain-boundary trap states and a zero-temperature Fermi distribution of carriers within those traps.⁴ The purpose of this paper is to calculate the admittance of a semiconductor bicrystal without those limitations.

In the next section the real and displacement currents associated with grain-boundary transport are calculated. The kinetics of charge trapping at the boundary are considered in detail because it is found that this charge modulates the real current under ac conditions, and this contributes strongly to the admittance. Finally the frequency and voltage dependence is numerically calculated for two forms of the trap-state density.

CALCULATION

As in the previous treatment, the admittance is determined from the currents which flow in response to an applied voltage

$$V(t) = V_{dc} + V_0 e^{i\omega t}, \quad (1)$$

where $eV_0/kT \ll 1$, k is Boltzmann's constant, and T is the absolute temperature. Evaluation of the conservation of the charge equation at the edge of the right-hand-side depletion region (see Fig. 1) with the abrupt approximation yields two components for the total current flowing in the external circuit,

$$J = J_R + \dot{Q}_R. \quad (2)$$

In the above equation \dot{Q}_R is the time rate of change of the two-dimensional (2D) charge density at the depletion edge d_R and J_R is the total real current flowing in the right-hand-side depletion layer. The two terms in Eq. (2) will be evaluated separately.

To find \dot{Q}_R the expression

$$Q_R = [2\epsilon\epsilon_0 N_d (\phi_B + eV)]^{1/2} \quad (3)$$

is differentiated with respect to time, where $\epsilon\epsilon_0$ is the dielectric constant, N_d is the donor density, ϕ_B is the barrier height, and V is the applied voltage (see Fig. 1). The barrier height depends on both V and the magnitude of the net 2D charge density Q trapped at the grain boundary. In general, V and Q can vary independently so

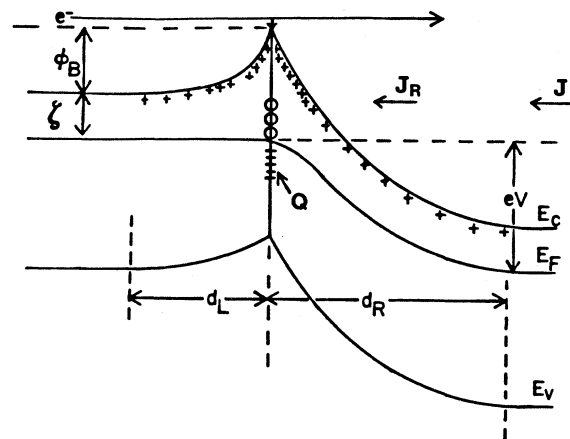


FIG. 1. Energy-band diagram for a bicrystal. This diagram schematically shows the essential features of an n -type semiconductor bicrystal with a voltage V applied across the grain boundary. Charge trapped at the boundary causes the potential barrier to form. Charge transfer into, out of, and directly across the grain boundary is assumed to occur by thermionic emission. The quantity eV_1 is the small unlabeled energy difference between the Fermi level at the boundary and in the left grain.

$$\dot{Q}_R = \left[\frac{\epsilon\epsilon_0 N_d}{2(\phi_B + eV)} \right]^{1/2} \times \left[\left[\frac{\partial\phi_B}{\partial Q} \right]_V \dot{Q} + \left[\frac{\partial\phi_B}{\partial V} \right]_Q \dot{V} + e\dot{V} \right]. \quad (4)$$

This may be simplified using the convenient expressions for the geometric capacitance per unit area of the right- and left-hand-side depletion regions, respectively,

$$C_R = [e^2\epsilon\epsilon_0 N_d / 2(\phi_B + eV)]^{1/2}, \quad (5)$$

$$C_L = [e^2\epsilon\epsilon_0 N_d / 2\phi_B]^{1/2}.$$

By adding Eq. (3) to its counterpart for the left-hand-side depletion charge density it can be easily shown that

$$\left[\frac{\partial\phi_B}{\partial Q} \right]_V = \frac{e}{C_L + C_R}$$

and

$$\left[\frac{\partial\phi_B}{\partial V} \right]_Q = -\frac{eC_R}{C_L + C_R}. \quad (6)$$

Equation (4) can now be written as

$$\dot{Q}_R = \frac{C_R}{C_L + C_R} \dot{Q} + \frac{C_L C_R}{C_L + C_R} \dot{V}. \quad (7)$$

Note that the second term contains the net series capacitance of the right- and left-hand-side depletion layers; this gives the high-frequency capacitance C_{hf} , which is also the geometrical capacitance.

To calculate the second current component J_R , thermionic emission is assumed for all currents over, into, and out of the grain-boundary barrier.^{4,15} The incident current densities of electrons with sufficient thermal energy to traverse the barrier left to right (LR) and right to left (RL) are given by

$$J_{i,LR} = A \exp[-(\zeta + \phi_B)/kT] \quad (8a)$$

and

$$J_{i,RL} = A \exp[-(\zeta + \phi_B + eV)/kT], \quad (8b)$$

where $A = A^* T^2$, A^* is the Richardson constant, and ζ is the energy separation between the Fermi level and the conduction-band minimum in the neutral crystallites (see Fig. 1). Also needed are expressions for the captured and emitted currents. For this purpose a distribution $N_T(E)$ of trap states is assumed to exist at the boundary. It is assumed that traps at all energies E exchange electrons only with conduction-band states, and not among themselves. This is clearly valid only in some dilute limit. As shown in Appendix A, the current densities into and out of the group of trap states within a range dE about an energy E are

$$dJ_{\text{capt}} = A\sigma N_T(E)dE [1 - f(E, E_F)] \times [1 + \exp(-eV/kT)] \exp[-(\zeta + \phi_B)/kT], \quad (9)$$

$$dJ_{\text{emis}} = 2A\sigma N_T(E)dE [1 - f(E, E_F)] \times \exp[-(\zeta + \phi_B + eV_1)/kT], \quad (10)$$

where σ is the capture cross section, assumed independent of E , $f(E, E_F)$ is the Fermi-distribution function for trapped electrons, and eV_1 is the small energy difference between the Fermi levels in the left (more negative) crystallite and the grain boundary. Under non-steady-state conditions the Fermi level at the grain boundary E_F (and consequently eV_1) will generally depend on the energy E of the trap states being described. The net positive current density in the right-hand-side depletion layer can now be calculated as

$$J_R = J_{i,LR} - J_{i,RL} + \frac{1}{2} \int dJ_{\text{emis}} - \int dJ_{\text{capt},LR}, \quad (11)$$

$$J_R = A \exp[-(\zeta + \phi_B)/kT] [1 - \exp(-eV/kT)] + A\sigma \exp[-(\zeta + \phi_B)/kT] \times \int N_T(E) [1 - f(E, E_F)] \times [\exp(-eV_1/kT) - 1] dE. \quad (12)$$

To evaluate Eq. (12) for an applied dc and ac voltage, it must be noted that ϕ_B , V_1 , and V all generally vary with time. Only $V(t)$ is known, see Eq. (1). If the magnitude of the ac signal is small, then $\phi_B(t)$ and $V_1(t)$ may be expanded about their dc values. Thus

$$\phi_B(t) = \phi_{B,dc} + \left[\frac{\partial\phi_B}{\partial V} \right]_Q \Delta V + \left[\frac{\partial\phi_B}{\partial Q} \right]_V \Delta Q = \phi_{B,dc} - \frac{eC_R}{C_L + C_R} \Delta V + \frac{e}{C_L + C_R} \Delta Q, \quad (13)$$

where $\Delta V = V_0 \exp(i\omega t)$, $\Delta Q = Q(t) - Q_{dc}$, and Eq. (6) has been used. The time dependence of V_1 is derived in Appendix B and is given by Eq. (B5) for the present case,

$$eV_1(E, t) = eV_{1,dc} + \frac{eC_R}{C_L + C_R} \Delta V - \frac{e}{C_L + C_R} \Delta Q + \frac{kT}{eN_T(E)f'(E)} \Delta q(E), \quad (14)$$

where $f'(E)$ is the dimensionless derivative of the Fermi function (see Appendix B), Q is charge/area, and $q(E)$ is charge/(area energy). Equations (13) and (14) contain the unknown quantity

$$\Delta Q(t) = \int \Delta q(E, t) dE. \quad (15)$$

To determine $\Delta Q(t)$ it is necessary to derive the rate equation for $q(E, t)$ and then solve it for the applied voltage $V(t)$ as the driving force. The details of this calculation are given in Appendix C where it is shown that the grain-boundary charge may be written as

$$\Delta Q(t) = C_Q \Delta V. \quad (16)$$

From Eqs. (C3), (C6), (C10), (C11), and (C14) it can be seen that the complex quantity C_Q contains the detailed information concerning the density of grain-boundary trap states $N_T(E)$ and the frequency dependence of their occupancy. The total current can now be calculated from Eqs. (2), (7), (12)–(14), and (16). For simplicity of presentation only the first line of Eq. (12) for J_R will be used (the full solution is given later). This amounts to a neglect

of the captured and emitted grain-boundary currents relative to the current flowing directly over the barrier. It is expected that this is a good approximation for many boundaries. In the only published measurement those currents were only a few percent of the total.⁴ After some algebraic manipulation the current can be written as

$$J = J_{dc} + \frac{J_{dc}e(C_R - C_Q)}{kT(C_L + C_R)}\Delta V + \frac{eA}{kT}e^{-(\xi + \phi_{Bdc} + eV_{dc})/kT}\Delta V + \frac{i\omega C_R C_Q}{C_L + C_R}\Delta V + \frac{i\omega C_L C_R}{C_L + C_R}\Delta V. \quad (17)$$

From this equation the complex admittance $Y = \Delta J / \Delta V$ is readily found to be

$$Y(\omega) = \frac{eJ_{dc}[C_R - C_Q(\omega)]}{kT(C_L + C_R)} + \frac{eA \exp[-(\xi + \phi_{Bdc} + eV_{dc})/kT]}{kT} + \frac{i\omega C_R C_Q(\omega)}{C_L + C_R} + \frac{i\omega C_L C_R}{C_L + C_R}. \quad (18)$$

Recognizing from Appendix C that $C_Q(0)$ is real, the dc conductivity is seen to be

$$G_{dc} = \frac{eJ_{dc}[C_R - C_Q(0)]}{kT(C_L + C_R)} + \frac{eA \exp[-(\xi + \phi_{Bdc} + eV_{dc})/kT]}{kT}. \quad (19)$$

Also, as noted earlier, the well-known expression for the high-frequency capacitance is

$$C_{hf} = \frac{C_L C_R}{C_L + C_R}. \quad (20)$$

Thus Eq. (18) can be rewritten as

$$Y(\omega) = G_{dc} + \frac{eJ_{dc}[C_Q(0) - C_Q(\omega)]}{kT(C_L + C_R)} + \frac{i\omega C_R C_Q(\omega)}{C_L + C_R} + i\omega C_{hf}. \quad (21)$$

A study of the origin, Eqs. (4) and (12), of the four terms in the above equation leads to their interpretation. The first term is due to current flowing over the grain-boundary barrier, and describes the expected dc loss. The second term is also from overbarrier currents, and represents the *indirect* effect of charge trapping at the grain boundary. This charge, which is partially out of phase with the applied voltage, causes ϕ_B to oscillate and thus modulate J_{dc} at a frequency ω . The third term comes from the *direct* effect of charge trapping. The capacitive part of this term, for example, is the geometric effect of storing charge in the grain boundary. This third term is exactly analogous to the admittance introduced by Nicollian and Goetzberger¹⁶ to describe the combined effect of the depletion-layer thickness and interface states in

metal-oxide-semiconductor (MOS) structures. The last term in Eq. (21) is simply due to the double depletion-layer capacitance which is measured at frequencies so high that grain-boundary charge cannot change.

If the full expression for J_R , Eq. (12), is used to compute the admittance, it can be shown that with a few approximations and much algebra the additional contribution to $Y(\omega)$ in Eq. (21) is

$$- \left[1 + \frac{e^2 N_{T1}(E_F)}{C_L + C_R} \right] \frac{C_Q(0) - C_Q(\omega)}{2\tau}, \quad (22)$$

where τ is defined in Appendix C, Eq. (C16), and N_{T1} is given by

$$N_{T1}(E_F) = \frac{1}{kT} \int N_T(E) e^{(E - E_F)/kT} f(E, E_F) dE. \quad (23)$$

To illustrate the voltage and frequency dependence of the calculated grain-boundary admittance the complete expression, Eqs. (21) and (22), has been evaluated numerically. Two energy distributions of trap states are treated, monoenergetic and uniformly distributed. The analytic forms for $C_Q(\omega)$ are derived in Appendix C. The procedure was to solve for the barrier height as a function of voltage from the charge balance equation,^{2,15}

$$(2\epsilon\epsilon_0 N_d)^{1/2} [\phi_B^{1/2} + (\phi_B + eV)^{1/2}] = e \int_{E_v}^{E_c} N_T(E) [f(E, E_F) - f(E, E_{FB})] dE, \quad (24)$$

where E_{FB} is the neutral Fermi level in the grain boundary. Then the conductance and capacitance ($\text{Re}[Y]$ and $\text{Im}[Y]/\omega$) can be calculated using assumed, but realistic values for the various parameters.

The simplest case is for the monoenergetic traps, because the admittance components can be written in the standard Debye form

$$G(\omega) = G_{dc} + \frac{\omega^2 \tau_2 C_D}{1 + \omega^2 \tau_2^2}, \quad (25a)$$

$$C(\omega) = C_{hf} + \frac{C_D}{1 + \omega^2 \tau_2^2}, \quad (25b)$$

where

$$C_D = \tau_2 C_2 \left[\frac{C_R}{\tau_2} + \frac{eJ_{dc}}{kT} - \frac{C_L + C_R + e^2 N_{T1}}{2\tau} \right] / (C_L + C_R), \quad (26)$$

and τ , τ_2 , C_2 , and N_{T1} are given in Appendix C. Since the frequency dependence of this form is well known, only the voltage dependence is discussed here. Figure 2 is a plot of the computed barrier height as a function of voltage for a bicrystal with $N_d = 3 \times 10^{17} \text{ cm}^{-3}$, $\epsilon = 8.5$, $\sigma = 2.5 \times 10^{-14} \text{ cm}^2$, $A^* = 29A/(\text{cm}^2 \text{K}^2)$, and grain-boundary trap states 0.60 eV below the conduction band with a density of $4 \times 10^{12} \text{ cm}^{-2}$. These parameters are appropriate to grain boundaries in ZnO varistors.^{9,12} At zero bias, the trap states are about half-filled. As V increases the empty states begin to fill, but the barrier

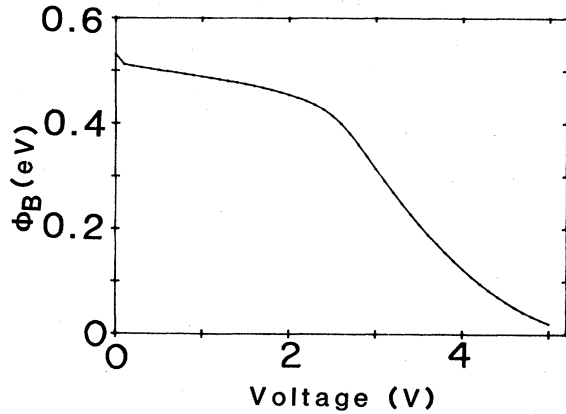


FIG. 2. Barrier height versus voltage for a monoenergetic density of grain-boundary trap states. These values were obtained by solving Eq. (24) using parameter values listed in the main text.

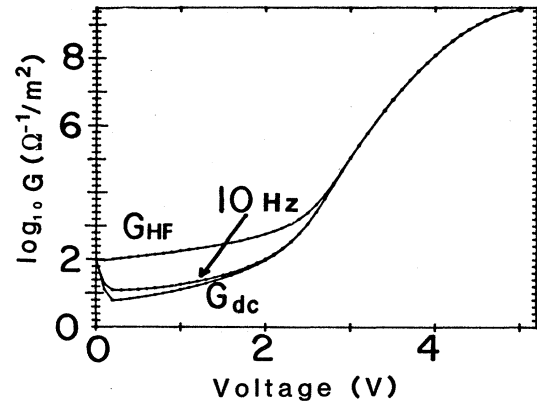


FIG. 5. Conductance versus voltage. This is the calculated conductance for the same bicrystal parameters used for Figs. 2-4.

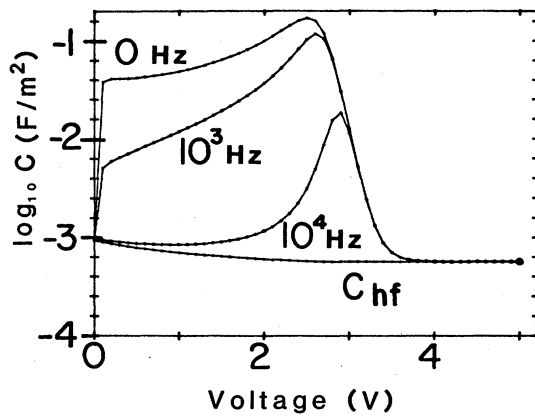


FIG. 3. Capacitance versus applied voltage. These are results of calculations for a grain boundary with a monoenergetic density of trap states. The variation of ϕ_B is given in Fig. 2. The high- and low-frequency limits are shown along with curves for two intermediate frequencies.

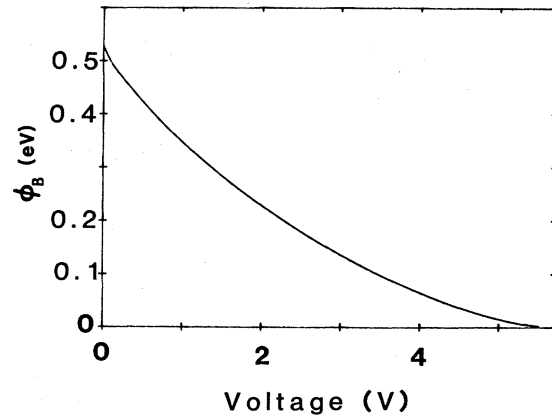


FIG. 6. Barrier height versus voltage for a uniform density of grain-boundary trap states. The dependence in this case is more uniform than that shown in Fig. 2.

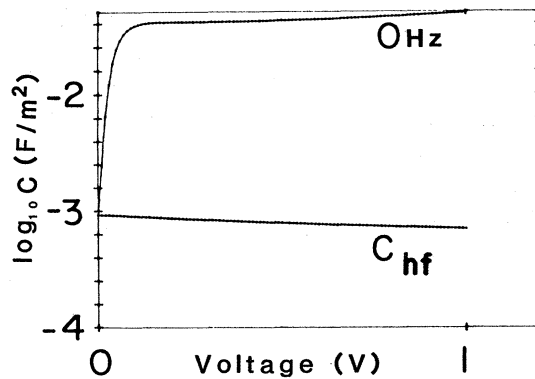


FIG. 4. Capacitance versus voltage. This is an expansion of the low-voltage part of Fig. 3.

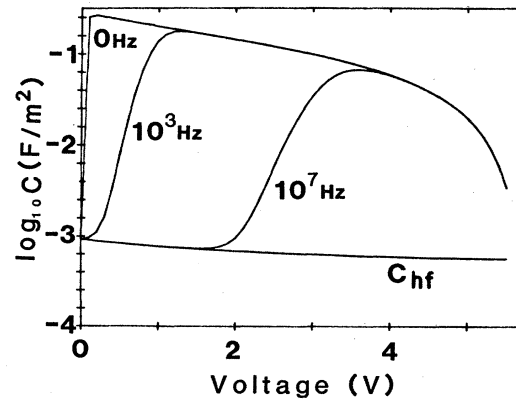


FIG. 7. Capacitance versus applied voltage. These are curves calculated for the same bicrystal parameters used for Fig. 6. The differences between these curves and those of Fig. 3 are due to the different energy distribution of grain-boundary trap states.

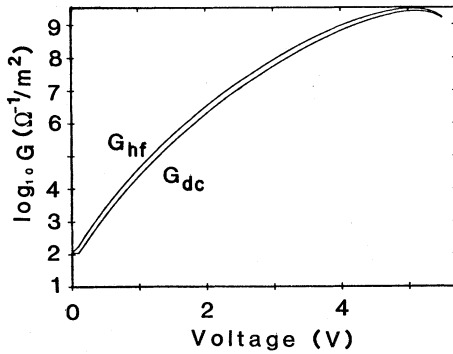


FIG. 8. Conductance versus voltage. These curves are calculated for the same parameters used in Figs. 6 and 7.

height is nearly pinned by the high density of states. Only when the trap states are almost all filled does the barrier height decrease significantly. The capacitance for this bicrystal is shown in Fig. 3. The value of C_{hf} shows a monotonic decline as expected, while the low-frequency capacitance rises immediately from C_{hf} with small applied voltage and then falls again near 2.5 V. This low voltage increase has been observed experimentally⁴ and is shown in more detail in Fig. 4. The decrease near 2.5 V is caused by the filling of the grain-boundary traps; without many empty states there is little charge exchange, and the barrier height oscillates in phase with the applied voltage. At intermediate frequencies the effect of a voltage-dependent time constant τ_2 is seen. From Eqs. (C16) and (C22) the voltage-dependent terms are ϕ_B and $f(E_T, E_F)$. At low voltage the value of τ is largest. For the example of 10^4 Hz, the value of $\omega\tau$ is greater than unity there. With increasing voltage $\omega\tau$ decreases and the capacitance curve moves toward the low-frequency limit. The variation of conductance with voltage is given in Fig. 5. The low bias decrease of G_{dc} is due to the sub-Ohmic behavior of J_{dc} induced by the nearly constant ϕ_B .² The high- and low-frequency curves merge for the same reason given above for the capacitance.

The second set of calculations are for a grain boundary in which the traps are uniformly distributed in energy. To illustrate the differences caused by the form of $N_T(E)$, the bicrystal parameters were chosen to be the same as those above except N_T was adjusted to provide the same number of empty states at equilibrium. The calculated $\phi_B(V)$ curve is shown in Fig. 6. The decrease is more uniform than shown in Fig. 2 because there is not a high density of states at one energy to pin E_F . This yields a capacitance-voltage relationship given in Fig. 7. The same general features seen for the monoenergetic trap case are again observed. However, because τ is changing more uniformly with voltage, the intermediate-frequency curves are more uniformly distributed along the voltage axis. In Fig. 7 a voltage increase of 2 V causes the transition frequency to shift by four decades while in Fig. 3 it shifts only by one decade. Also, since there are empty trap states available at all voltages, the low-frequency capacitance remains much larger than C_{hf} until the barrier height is nearly 0. The conductance is plotted in Fig. 8,

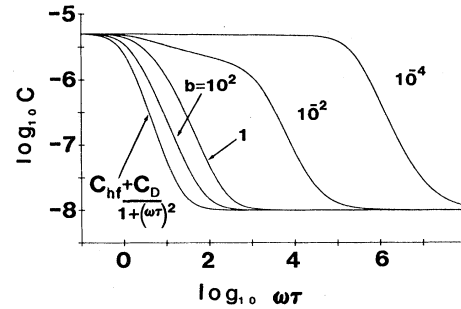


FIG. 9. Frequency dependence of capacitance. These curves illustrate how the bicrystal capacitance can vary with frequency. For ease of comparison the curves have all been normalized to the same high- and low-frequency values, and hence the capacitance units are completely arbitrary. The curve on the extreme left side is the standard Debye dependence which results from a monoenergetic density of grain-boundary states, Eq. (25b). The other four curves are for a bicrystal whose grain-boundary states are uniformly distributed in energy. The different curves result from different values of the parameter b which is defined by Eq. (C26).

and it differs considerably from that shown in Fig. 5. Thus the actual form of the density of trap states can strongly affect the details of grain-boundary admittance.

The frequency dependence of the capacitance for both forms of $N_T(E)$ is illustrated in Fig. 9. Plotted there is the calculated capacitance normalized to the same high- and low-frequency values for easier comparison. The abscissa is $\omega\tau_2$ [see Eq. (C22)] for the curve on the extreme left which pertains to the Debye form of the monoenergetic case. The other curves are plotted against $\omega\tau$ [see Eq. (C16)] for the uniform $N_T(E)$ case. Different values of the parameter $b = \tau_1/\tau$ [Eq. (C25)] were used to generate the four curves. For the curves with $b = 10^2$, 1, and 10^{-2} only the J_{dc} term in Eq. (21) contributes significantly to the frequency dependence. For $b = 10^{-4}$ the third term in Eq. (21) dominates. At large values of b the curves are almost Debye-type; however, there is always a larger frequency range needed to make the transition from low- to high-frequency values. This spread is expected from the thermal smearing of occupied trap levels around the Fermi level which causes a distribution of τ values. This spread did not occur (the curves were Debye-type) when the calculation was previously made with the $T=0$ approximation for the Fermi function.

CONCLUSIONS

The admittance of a semiconductor bicrystal containing a grain-boundary potential barrier has been calculated for an arbitrary density of grain-boundary states occupied by a Fermi distribution of majority carriers. Two particular forms for the density of states were chosen to illustrate the voltage and frequency dependence of the admittance. Numerical evaluation of the conductance and capacitance showed that their variations depend strongly on the form of the trap-state distribution.

APPENDIX A: CAPTURE AND EMISSION CURRENTS

The rate at which charge is captured by states at energy E to $E + dE$ depends on the flux of electrons incident on the grain boundary, the capture cross section of the traps, $\sigma(E)$, and the number of empty states, $N_T(E)dE[1 - f(E, E_F)]$. In general, under transient conditions the grain-boundary Fermi level E_F will depend on the energy E of the trap being described (see Appendix B for an explicit treatment). From Eq. (8)

$$dJ_{\text{capt}} = A\sigma(E)N_T(E)dE[1 - f(E, E_F)] \times [1 + \exp(-eV/kT)] \exp[-(\zeta + \phi_B)/kT]. \quad (\text{A1})$$

The current thermionically emitted from those same states within dE about E depends on the number of occupied states, $N_T(E)dEf(E, E_F)$, and on some average waiting time t_0 . Thus

$$dJ_{\text{emis}} = (e/t_0)N_T(E)dEf(E, E_F) \exp[-(E_g - E)/kT], \quad (\text{A2})$$

where E_g is the band-gap energy. However, using $E_g = \phi_B + E_F + eV_1 + \zeta$ in the grain boundary, it can be shown that

$$f(E, E_F) \exp[-(E_g - E)/kT] = [1 - f(E, E_F)] \exp[-(\zeta + \phi_B + eV_1)/kT], \quad (\text{A3})$$

where eV_1 is the Fermi-level difference between the grain boundary and the more negative grain. So now Eq. (A2) becomes

$$dJ_{\text{emis}} = (e/t_0)N_T(E)dE[1 - f(E, E_F)] \times \exp[-(\zeta + \phi_B + eV_1)/kT]. \quad (\text{A4})$$

At $V=0$, in equilibrium, $V_1=0$ and $dJ_{\text{capt}} = dJ_{\text{emis}}$ for each group of trap states. Thus

$$2A\sigma = e/t_0, \quad (\text{A5})$$

where σ and t_0 have been assumed to be independent of E . The emission current density then has a form similar to Eq. (A1),

$$dJ_{\text{emis}} = 2A\sigma N_T(E)dE[1 - f(E, E_F)] \times \exp[-(\zeta + \phi_B + eV_1)/kT]. \quad (\text{A6})$$

APPENDIX B: TIME DEPENDENCE OF $V_{1i}(t)$

Consider a boundary with M discrete trap-energy levels E_i of spatial density N_i , $i=1, M$. Then

$$eV_{1i}(t) = eV_{1i, \text{dc}} + \left[\frac{\partial V_{1i}}{\partial V} \right]_{Q_k} e\Delta V + e \left[\frac{\partial V_{1i}}{\partial Q_i} \right]_{V, Q_{j \neq i}} \Delta Q_i + e \sum_{\substack{j=1 \\ j \neq i}}^M \left[\frac{\partial V_{1j}}{\partial Q_j} \right]_{V, Q_{k \neq j}} \Delta Q_j, \quad (\text{B1})$$

where Q_i is the charge/area in the i th level. The last term

exists because, even though charge change in trap $j \neq i$ does not change the occupancy of trap i , it does change the barrier height and hence the level of the Fermi level for trap i relative to the grain Fermi level. It is also important to note that in general, for non-steady-state conditions, the occupancy of each trap is described by its own value of $V_{1i}(t)$.

To evaluate the partial derivatives, use

$$Q_i = eN_i[f(E_i, E_{Fi}) - f(E_i, E_{FB})], \quad (\text{B2})$$

where E_{Fi} is the Fermi level that determines the occupancy of the i th level and E_{FB} is the position of the neutral Fermi level in the grain boundary.^{2,15} Then

$$1 = \frac{eN_i}{kT} f'_i \left[\frac{\partial(\phi_B + eV_{1i})}{\partial Q_i} \right]_{V, Q_{j \neq i}}, \\ 0 = \left[\frac{\partial(\phi_B + eV_{1i})}{\partial Q_j} \right]_{V, Q_{k \neq j}}, \\ 0 = \left[\frac{\partial(\phi_B + eV_{1i})}{\partial eV} \right]_{Q_k},$$

where $f(x) = 1/(1 + e^x)$, $f' = \partial f/\partial x = -f(x)f(-x)$, and

$$x_i = \frac{E_i - E_{Fi}}{kT} = \frac{E_i - (E_g - \zeta - \phi_B - eV_{1i})}{kT} \\ = \frac{E_i - E_g + \zeta}{kT} + \frac{\phi_B + eV_{1i}}{kT}.$$

From these equations plus Eq. (6) one has

$$e \left[\frac{\partial V_{1i}}{\partial Q_i} \right]_{V, Q_{j \neq i}} = \frac{kT}{eN_i f'_i} - \frac{e}{C_L + C_R}, \\ e \left[\frac{\partial V_{1i}}{\partial Q_j} \right]_{V, Q_{k \neq j}} = -\frac{e}{C_L + C_R}, \\ \left[\frac{\partial V_{1i}}{\partial V} \right]_{Q_k} = \frac{C_R}{C_L + C_R}.$$

Thus

$$eV_{1i}(t) = eV_{1i, \text{dc}} + \frac{C_R}{C_L + C_R} e\Delta V \\ + \left[\frac{kT}{eN_i f'_i} - \frac{e}{C_L + C_R} \right] \Delta Q_i \\ - \sum_{\substack{j=1 \\ j \neq i}}^M \frac{e}{C_L + C_R} \Delta Q_j. \quad (\text{B3})$$

But $\sum_{j=1}^M \Delta Q_j = \Delta Q$, so

$$eV_{1i}(t) = eV_{1i, \text{dc}} + \frac{C_R}{C_L + C_R} e\Delta V \\ - \frac{e}{C_L + C_R} \Delta Q + \frac{kT}{eN_i f'_i} \Delta Q_i. \quad (\text{B4})$$

To connect this expression to one for a continuous distribution of trap energies, the index i is associated with an energy E ,

$$\Delta Q_i \rightarrow dE \Delta q(E) \quad \text{and} \quad N_i \rightarrow dE N(E) \quad \text{and} \quad V_{1i} \rightarrow V_1(E).$$

Note that Q is charge/area, but $q(E)$ is charge/(area energy). Thus for the case of states distributed continuously in energy,

$$eV_1(E,t) = eV_{1,dc}(E) + \frac{C_R}{C_L + C_R} e\Delta V - \frac{e}{C_L + C_R} \Delta Q + \frac{kT}{eN(E)f'(E)} \Delta q(E). \quad (B5)$$

Furthermore, in steady state (dc) the capture and emission currents must be equal. Hence from Eqs. (9) and (10),

$$eV_{1,dc}(E) = -\ln \left[\frac{1 + e^{-eV/kT}}{2} \right] = eV_{1,dc}. \quad (B6)$$

In steady state all trap levels are governed by the same $V_{1,dc}$.

APPENDIX C: CALCULATION OF C_Q

The quantity $\Delta Q(t)$ is found by writing the time-dependent equation for $q(E,t)$, integrating over energy to get an equation for $Q(t)$, and then solving it specifically for the voltage variation given by Eq. (1). The time rate of change of grain-boundary trap charge in an interval dE about E is determined from Eqs. (9) and (10) to be

$$\begin{aligned} \dot{q}(E,t)dE &= dJ_{\text{capt}} - dJ_{\text{emis}} \\ &= A\sigma N_T(E)[1 - f(E, E_F)] \exp[-(\zeta + \phi_B)/kT] \\ &\quad \times [1 + \exp(-eV/kT) - 2 \exp(-eV_1/kT)] dE. \end{aligned} \quad (C1)$$

By expanding ϕ_B , V_1 , and V about their dc values [Eqs. (13) and (14)], this equation may be set into the following form:

$$\dot{q}(E,t) = -p(E)\Delta Q(t) - r(E)\Delta q(E,t) - u(E)\Delta V, \quad (C2)$$

where

$$p(E) = eD(E)/kT(C_L + C_R), \quad (C3)$$

$$r(E) = -D(E)/[eN_T(E)f'(E)]_{dc}, \quad (C4)$$

$$u(E) = eD(E)[f_v - C_R/(C_L + C_R)]/kT, \quad (C5)$$

$$D(E) = \{2A\sigma N_T(E)[1 - f(E, E_F)] \times \exp[-(\zeta + \phi_B + eV_1)/kT]\}_{dc}, \quad (C6)$$

$$f_v = 1/[1 + \exp(eV/kT)]. \quad (C7)$$

Equation (C2) is most easily solved using Laplace-transform techniques. The integrated Laplace transform can be written as

$$\begin{aligned} \bar{Q}(s) &\left[1 + \int \frac{p(E)dE}{r(E)+s} \right] \\ &= \int \frac{dE}{r(E)+s} \left[q(E,0) + p(E) \frac{Q_{dc}}{s} \right. \\ &\quad \left. + r(E) \frac{q_{dc}(E)}{s} - \frac{u(E)V_0}{s-i\omega} \right], \end{aligned} \quad (C8)$$

where $\bar{Q}(s)$ is the transform of $Q(t)$. Only the long-term ac and dc solutions are desired, and so transient terms in the solution will be ignored. Hence only the poles at $s=0$ and $i\omega$ will be used. The inverse Laplace transform of the two terms containing dc quantities is

$$\begin{aligned} \lim_{s \rightarrow 0} \frac{1}{1+P(s)} \int \frac{dE [p(E)Q_{dc} + r(E)q_{dc}(E)]}{r(E)+s} \\ = Q_{dc} \left[\frac{P(0)+1}{1+P(0)} \right] = Q_{dc}, \end{aligned} \quad (C9)$$

where

$$P(s) = \int \frac{p(E)dE}{r(E)+s}. \quad (C10)$$

Using a similar definition,

$$U(s) = \int \frac{u(E)dE}{r(E)+s}, \quad (C11)$$

the quantity $\Delta Q(t)$ may be written from Eqs. (C8), (C10), and (C11) as

$$Q(t) - Q_{dc} = L^{-1} \left[\frac{-V_0}{(s-i\omega)} \frac{U(s)}{[1+P(s)]} \right], \quad (C12)$$

where L^{-1} indicates the inverse transform. Thus

$$\Delta Q(t) = \lim_{s \rightarrow i\omega} \left[\frac{-U(s)V_0 e^{i\omega t}}{1+P(s)} \right] \equiv C_Q(\omega)\Delta V, \quad (C13)$$

where

$$C_Q(\omega) = \lim_{s \rightarrow i\omega} \left[\frac{-U(s)}{1+P(s)} \right]. \quad (C14)$$

The quantity $C_Q(\omega)$ can be analytically evaluated for several forms of $N_T(E)$. This is done here for two cases so that the results may be used to calculate $Y(\omega)$ in the main part of this paper. For these evaluations it is useful to note that $U(s)$ and $P(s)$ contain the same integral,

$$I(s) = \int_{E_b}^{E_c} \frac{N_T(E)f(E)f(-E)}{1+s\tau f(E)} dE, \quad (C15)$$

where τ has been defined as

$$\tau = \{(e/2A\sigma) \exp[(\zeta + \phi_B + eV_1)/kT]\}_{dc}. \quad (C16)$$

Using

$$K = C_R - f_v(C_L + C_R), \quad (C17)$$

one can write

$$C_Q(\omega) = \lim_{s \rightarrow i\omega} \left[\frac{KI(s)}{(C_L + C_R)kT/e^2 + I(s)} \right]. \quad (C18)$$

1. Case A: $N_T(E) = N_{T0}\delta(E - E_T)$

This is the case for a monoenergetic set of trap states with 2D density of N_{T0} . From Eq. (C15) it is readily seen that

$$I(s) = \frac{N_{T0}f(E_T)f(-E_T)}{1+s\tau f(E_T)} \quad (\text{C19})$$

After some algebraic manipulation it can be shown that

$$C_Q(\omega) = \frac{C_2}{1+i\omega\tau_2}, \quad (\text{C20})$$

where

$$C_2 = \frac{KN_{T0}f(E_T)f(-E_T)}{N_{T0}f(E_T)f(-E_T) + (C_L + C_R)kT/e^2} \quad (\text{C21})$$

and

$$\tau_2 = \frac{\tau f(E_T)(C_L + C_R)kT/e^2}{N_{T0}f(E_T)f(-E_T) + (C_L + C_R)kT/e^2}. \quad (\text{C22})$$

2. Case B: $N_T(E) = N_T$

This is the case when there exists the same spatial density of trap states within all equal energy ranges above the

equilibrium Fermi level. After some straightforward variable changes, $I(s)$ can be set into the form of a standard integral, and be evaluated as

$$I(s) = \frac{N_T kT}{s\tau} \ln \left[\frac{1+s\tau f(E_v)}{1+s\tau f(E_c)} \right]. \quad (\text{C23})$$

To a high degree of accuracy, $f(E_c) = 0$ and $f(E_v) = 1$, so

$$I(s) = \frac{N_T kT}{s\tau} \ln(1+s\tau). \quad (\text{C24})$$

Then it can be shown that

$$C_Q(\omega) = \frac{K \ln(1+i\omega\tau)}{i\omega\tau b/2 + \ln(1+i\omega\tau)}, \quad (\text{C25})$$

where K was defined in Eq. (C17), and

$$b = 2(C_L + C_R)/e^2 N_T. \quad (\text{C26})$$

- ¹C. H. Seager and T. G. Castner, *J. Appl. Phys.* **49**, 3879 (1978).
²G. E. Pike and C. H. Seager, *J. Appl. Phys.* **50**, 3414 (1979).
³C. H. Seager and G. E. Pike, *Appl. Phys. Lett.* **35**, 709 (1979).
⁴C. H. Seager and G. E. Pike, *Appl. Phys. Lett.* **37**, 747 (1980).
⁵M. J. Cohen, M. D. Paul, D. L. Miller, J. R. Waldrop, and J. S. Harris, *J. Vac. Sci. Technol.* **17**, 899 (1980).
⁶C. H. Seager and G. E. Pike, *Appl. Phys. Lett.* **40**, 471 (1982).
⁷W. Siegel, G. Kuhnel, and E. Ziegler, *Phys. Status Solidi A* **64**, 249 (1981).
⁸J. W. Orton, B. J. Goldsmith, M. J. Powell, and J. A. Chapman, *Appl. Phys. Lett.* **37**, 557 (1980).

- ⁹G. E. Pike, *Mater. Res. Soc. Proc.* **5**, 369 (1982).
¹⁰H. Ihrig and W. Puschert, *J. Appl. Phys.* **48**, 3081 (1977).
¹¹R. Einzinger, *Adv. Ceram.* **1**, 359 (1981).
¹²L. M. Levinson and H. R. Philipp, *J. Appl. Phys.* **47**, 1117 (1976).
¹³L. F. Lou, *Appl. Phys. Lett.* **36**, 570 (1980).
¹⁴J. Werner and H. Strunk, *J. Phys. (Paris) Colloq.* **43**, C1-89 (1982).
¹⁵G. E. Pike and C. H. Seager, *Adv. Ceram.* **1**, 53 (1981).
¹⁶E. H. Nicollian and A. Goetzberger, *Appl. Phys. Lett.* **7**, 216 (1965).